

# Small inertial measurement units - sources of error and limitations on accuracy

Michael E. Hoenk

Center for Space Microelectronics Technology  
Jet Propulsion Laboratory  
California Institute of Technology  
4800 Oak Grove Drive  
Pasadena, California, 91109

## ABSTRACT

Limits on the precision of small accelerometers for inertial measurement units are enumerated and discussed. Scaling laws and errors which affect the precision are discussed in terms of tradeoffs between size, sensitivity, and cost. Thermal noise and displacement transducer sensitivity constrain the size of an accelerometer for a given sensitivity, and error correction for inertial navigation leads to a tradeoff between cost and precision. Emphasis is placed on micromachined silicon accelerometers as a potential technology for manufacturing low cost, precision sensors, and sample calculations are given to illustrate the principles.

## 1. INTRODUCTION

Smaller inertial measurement units promise new applications, lower cost systems, and, within the context of the design constraints of particular applications, better performance. This is exemplified by a micro-seismometer developed at JPL for applications in which size is a critical parameter.<sup>1</sup> The small size of this instrument has enabled its deployment at the bottom of a borehole 7000 ft beneath the Earth's surface, and by a micro-rover designed for traveling the surface of Mars. Despite its small size, this instrument achieved a sensitivity of  $10^{-9} \text{ g}/\sqrt{\text{Hz}}$  over a 40 Hz bandwidth. A different set of constraints applies to the design of inertial grade accelerometers, which affect the ability to obtain such high sensitivity in an inertial measurement unit. Although the principles are the same, these constraints dictate a different mechanical design and consequently different performance. For example, the larger bandwidth and the larger dynamic range required for inertial grade accelerometers result in higher noise and more robust design than for sensitive seismometers.

In this paper, the limits on the precision of small accelerometers for inertial measurement units are considered, with the understanding that similar principles can be applied to the analysis of small gyroscopes. In order to evaluate the possibility of adapting the technology which led to the success of JPL's micro-seismometer program to inertial grade accelerometers, the tradeoffs between size, sensitivity, and cost are considered. The approach considered for achieving small size in a low-cost accelerometer is silicon micromachining.<sup>2,3</sup> Silicon micromachining has enabled the mass production of small, low cost sensors for a variety of applications, in some cases incorporating integrated electronics for signal conditioning. There is already a large commercial market for micromachined accelerometers, which are used as crash sensors in automobile airbag systems. If low-cost, low mass precision accelerometers and gyroscopes were fabricated using micromachining techniques, inexpensive inertial navigation systems could be manufactured for use in applications for which cost was previously a prohibitive factor. Scaling laws related to thermal noise limit the sensitivity of these sensors as the size

is reduced, and error correction required for inertial navigation dictates a tradeoff between cost and precision.

## 2. NOISE AND ACCUMULATED ERROR IN INTEGRATED ACCELERATION

The first consideration in discussing the scaling of accelerometers is the relationship between the accumulated error and the noise floor of the instrument. Figure 1 shows a schematic representation of an accelerometer, as it might be designed using silicon micromachining. The mechanical design consists of a proof mass,  $m$ , supported by a spring with spring constant  $k$ . The separation between the proof mass and the package,  $s$ , is the measured quantity which is used to determine the component of the acceleration vector along the sensitive axis of the accelerometer. The relationship between the motion of the proof mass and the acceleration is given by

$$\frac{d^2s}{dt^2} + \frac{\omega_r}{Q} \frac{ds}{dt} + \omega_r^2 s = a(t) \quad (1)$$

where  $\omega_r (= \sqrt{k/m})$  is  $2\pi$  times the resonant frequency, and  $Q$  is the quality factor of the suspension.

In order to determine the position as a function of time, the acceleration must be integrated twice. Any error in the measured acceleration is also integrated, leading to accumulation of error in the

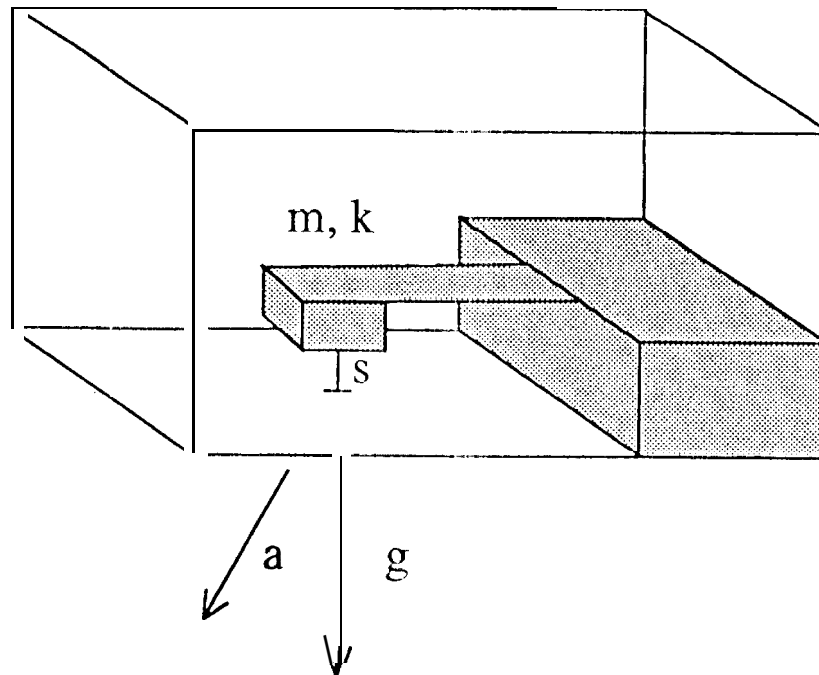


Figure 1: Schematic of a micromachined accelerometer. A proof mass,  $m$ , is supported by a spring with spring constant,  $k$ . The separation between the proof mass and the package is measured, and used to determine one component of the time-dependent acceleration vector.

calculated position. While sophisticated filters exist for minimizing this error,<sup>4</sup> a simple calculation is sufficient to **relate** the noise floor of the instrument to the accumulated error. The noise floor should be given in terms of acceleration noise, with units of  $g/\sqrt{\text{Hz}}$ , in order to compare it with thermal noise equivalent acceleration (TNEA) as defined in the next section. Although thermal noise is, in general, frequency dependent, **it will** be shown that the TNEA of an accelerometer is independent of frequency. **Integration** of the square of this noise over the frequency band of interest gives the mean square noise in that bandwidth. The average position error as a function of time can be estimated by

$$\Delta x = \frac{1}{2} \delta a_{\text{rms}} t^2, \quad (2)$$

where  $\Delta x$  is the position error,  $\delta a_{\text{rms}}$  is the root mean square error in acceleration, and  $t$  is the integration time. The root mean square error is related to an average power spectral density over the measured bandwidth,  $\Delta f$ , by

$$\delta a = \frac{\delta a_{\text{rms}}}{\sqrt{\Delta f}} \quad (3)$$

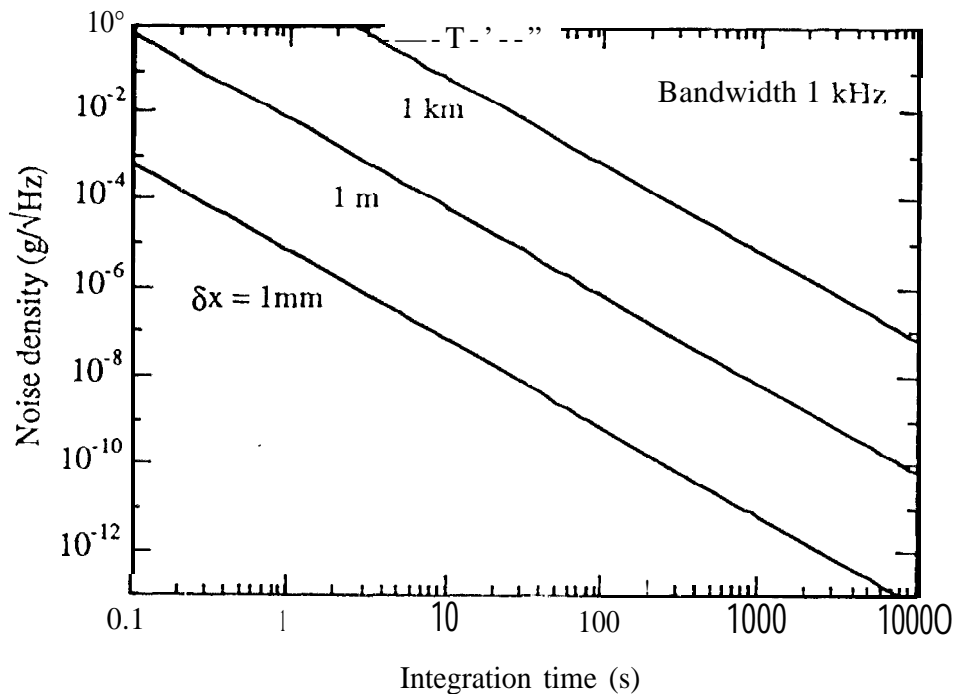


Figure 2: Accumulated error in integrated acceleration measured in a 1 kHz bandwidth. Plots of constant position error are shown on a graph of noise density vs. integration time.

Given these assumptions, it is possible to calculate the integrated error,  $A_x$ , as a function of bandwidth, noise density (in  $g/\sqrt{\text{Hz}}$ ), and integration time. Figure 2 shows a plot of the integrated error, assuming a 1 kHz bandwidth. Contours of constant position error are plotted on a graph of noise equivalent acceleration versus integration time. Given an error tolerance and an integration time, the plot can be used to determine the maximum noise density which will keep the accumulated error below the tolerance. As an example, an accelerometer with a bandwidth of 1 kHz and a noise floor below  $10^{-7} g/\sqrt{\text{Hz}}$  will allow determination of the position to within 1 m for integration times of up to approximately 4 minutes. This noise figure puts constraints on the accelerometer design due to thermal noise related scaling laws, considered in the next section.

### 3. THERMAL NOISE AND ACCELEROMETER SCALING

The ultimate sensitivity achievable by any accelerometer based on measured displacement of a spring-supported mass is determined by thermal noise in the proof mass motion.<sup>5</sup> This noise source is indistinguishable from signals due to real acceleration, and leads to a fundamental scaling law relating the sensitivity to the accelerometer design. Thermal motion of the proof mass, analogous to Johnson noise in a resistor, can be calculated from the fluctuation-dissipation theorem applied to a simple mass/spring model of an accelerometer,

$$|s| = \sqrt{\frac{4k_b T \omega_r}{mQ\{(\omega^2 - \omega_r^2)^2 + \frac{\omega^2 \omega_r^2}{Q^2}\}}} \quad \text{for } k_b T \gg \hbar \omega \quad (4)$$

where  $s$  is the noise density (in  $m/\sqrt{\text{Hz}}$ ) as a function of frequency,  $\omega$ ,  $T$  is the absolute temperature,  $k_b$  is Boltzmann's constant,  $\omega_r$  is  $2\pi$  times the resonant frequency of the suspension,  $m$  is the proof mass, and  $Q$  is the quality factor of the suspension. In order to relate this noise to the acceleration signal, we use the frequency dependent responsivity of the suspension to an applied acceleration, found by solving equation 1 in frequency space:

$$\left| \frac{s}{a} \right| = \frac{1}{\sqrt{(\omega^2 - \omega_r^2)^2 + \frac{\omega^2 \omega_r^2}{Q^2}}} \quad (5)$$

The thermal noise equivalent acceleration is defined as the ratio of the thermal motion of the proof mass (equation 4) to the responsivity of the accelerometer to acceleration (equation 5),

$$\text{TNEA} = \sqrt{\frac{4k_b T \omega_r}{mQ}} \quad \text{for } k_b T \gg \hbar \omega \quad (6)$$

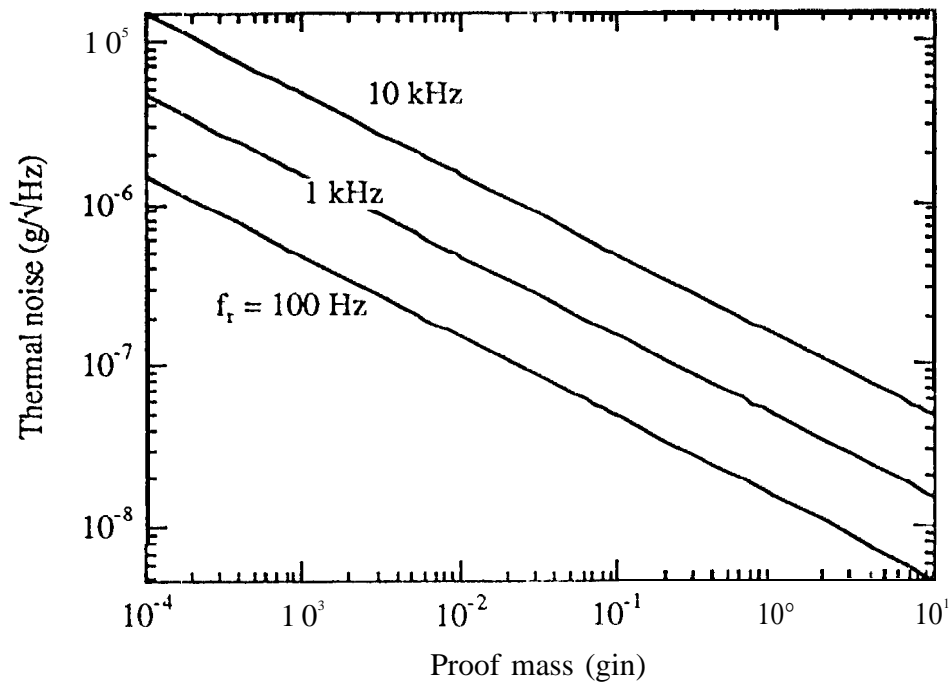


Figure 3: Thermal noise equivalent acceleration as a function of proof mass for three different resonant frequencies, for a critically damped accelerometer. Thermal noise decreases as proof mass increases.

The thermal noise equivalent acceleration is independent of frequency, subject to the constraint given in equation 6. However, this constraint is met for all frequencies of interest (at  $T = 300 \text{ K}$ ,  $k_b T < \hbar \omega$  for  $f < 6 \times 10^{12} \text{ Hz}$ ).

As an example of the effect of thermal noise on accelerometer design, assume that a micromachined sensor must be designed to have a noise floor below  $10^{-7} \text{ g}/\sqrt{\text{Hz}}$ , as discussed in the last section. As will become apparent, this is a stringent requirement for a micromachined accelerometer, and several constraints exist which affect the feasibility of using silicon micromachining to fabricate an accelerometer with this precision. For the purpose of argument, assume that the inertial navigation application requires a bandwidth of 1 kHz, and that the accelerometer suspension must be critically damped in order to avoid errors due to non-linearity of the responsivity near the resonance frequency. Choosing a resonant frequency of 1 kHz, a measurement bandwidth of 1 kHz, a Q of 0.5 (critically damped), and setting the thermal noise to  $10^{-7} \text{ g}/\sqrt{\text{Hz}}$ , figure 3 gives a required proof mass of 0.3 gm. This is a relatively large proof mass for a micromachined structure. A typical silicon wafer is about 0.5 mm thick, which leads to proof mass dimensions of 1.6 cm x 1.6 cm x 0.05 cm.

To complete the mechanical design, the dimensions of the silicon spring which supports this proof mass must be calculated. For simplicity, assume that the spring will be configured as a simple cantilever made from silicon, with a rectangular cross section. The cantilever will be characterized by a width,  $w$ , a length,  $\ell$ , and a thickness,  $t$ . The spring constant corresponding to these dimensions is given by<sup>6</sup>

$$k = \frac{E w t^3}{4 \ell^3} \quad (7)$$

where  $E$  is Young's modulus (approximately  $1.9 \times 10^{11} \text{ N/m}^2$  for silicon). In order to minimize cross sensitivity of the accelerometer, choose  $w = 100 \text{ t}$ . If  $t = 10 \text{ } \mu\text{m}$ , which is reasonable for a micromachined structure, then  $w = 1 \text{ mm}$ . Using the definition of the resonant frequency ( $k = \omega_r^2 m$ ), and the design value of  $f_r = 1 \text{ kHz}$ , we calculate that  $\ell = 2.7 \text{ mm}$ . Finally, the maximum strain in this spring structure is given by<sup>6</sup>

$$\sigma = \frac{6 W \ell}{w t^2} \quad (8)$$

where  $W$  is the load, which depends on orientation in the gravitational field and acceleration. For design purposes, we will calculate the maximum strain when the accelerometer is at rest with its sensitive axis aligned with Earth's gravitational field ( $W = mg$ , where  $m$  is the proof mass). In this case,  $\sigma = 5 \times 10^8 \text{ N/m}^2$ , which is to be compared to the yield strength of silicon<sup>7</sup>,  $7 \times 10^9 \text{ N/m}^2$ . Given that the accelerometer may experience much larger signals than the static  $1 \text{ g}$  gravitational field assumed here, this structure is rather fragile, and will require mechanical stops to prevent motion of the proof mass beyond the elastic limit of the silicon spring. However, using formula 10 (given in the next section), we can calculate that the spring will be deflected by only  $0.25 \text{ } \mu\text{m}$  in a  $1 \text{ g}$  gravitational field, making it difficult to fabricate mechanical stops which are close enough to the suspension to prevent the spring from breaking under conditions of high acceleration. One solution is to increase the thickness of the cantilever, which will increase the overall size of the device. Keeping the same aspect ratio of width to thickness, we can show that the length of the spring scales as  $t^{4/3}$ , and the maximum strain scales as  $t^{-5/3}$ . Therefore, increasing the thickness and width of the cantilever by a factor of 5 will require that the length of the cantilever be  $2.3 \text{ cm}$ , a substantial increase in the required size of the device. This will reduce the maximum strain in a  $1 \text{ g}$  gravitational field to  $3 \times 10^7 \text{ N/m}^2$ , in which case the structure would reach the yield strength of silicon at an acceleration of approximately  $200 \text{ g}$ .

Rather than accepting a much larger suspension  $m$  increase the robustness, the proof mass can be reduced. It is possible to reduce the proof mass without increasing the thermal noise by increasing the  $Q$  of the suspension, although this may lead to additional problems in the measurement. The relationship between the required proof mass and the thermal noise is illustrated graphically in figure 4, which is plotted for a  $1 \text{ kHz}$  resonant frequency. Most inertial grade accelerometers operate with a critically damped suspension in order to avoid distortion of the data near the resonant frequency and to minimize vibration rectification errors. Nevertheless, the design goals in this example have led to a relatively large, fragile device, a problem which can be alleviated by reducing the proof mass and redesigning the suspension. If we were to increase  $Q$  and reduce  $m$  in order to leave the thermal noise unchanged, and we were also to leave  $w$ ,  $t$ , and the resonant frequency unchanged, we can show that the maximum strain decreases inversely with  $Q$  to the  $2/3$  power:

$$\frac{\sigma}{\sigma_0} = \left(\frac{Q_0}{Q}\right)^{2/3}, \quad (9)$$

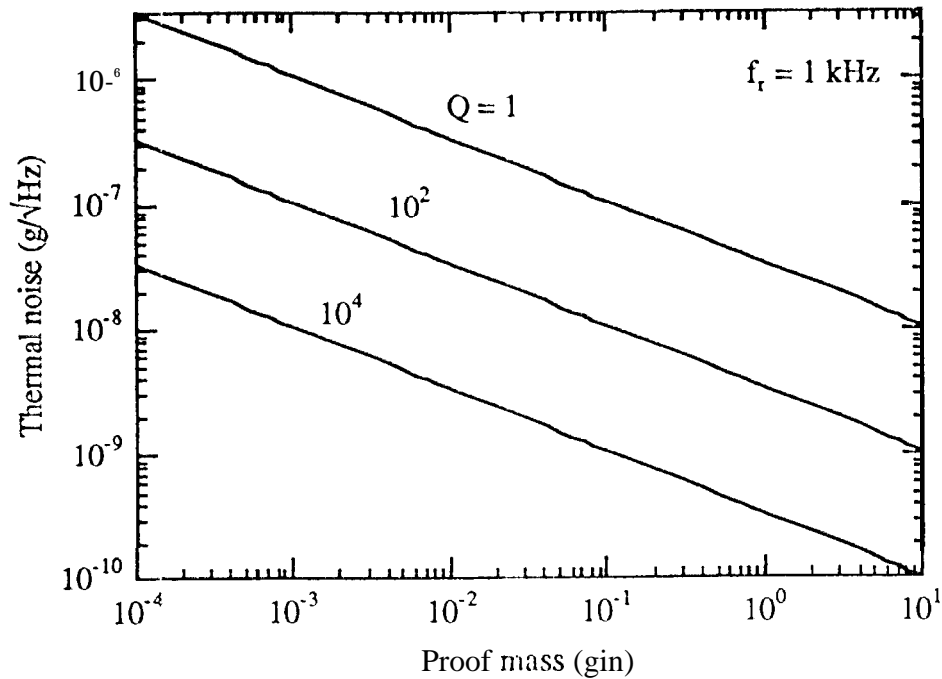


Figure 4: Thermal noise equivalent acceleration as a function of proof mass for three different values of the quality factor,  $Q$ , for a 1 kHz resonant frequency. Thermal noise decreases as  $Q$  increases.

where  $\sigma$  and  $Q$  are the new values and  $\sigma_0$  and  $Q_0$  are the old values of the maximum strain and the quality factor. By increasing the  $Q$  from 0.5 to 10, for example, the maximum strain in the spring could be reduced to  $3.2 \times 10^7 \text{ N/m}^2$ , corresponding to a maximum acceleration of approximately 200 g. Since the product of mass and  $Q$  appears in the formula for thermal noise, the mass will then scale from 0.3 gm down to 0.015 gm, and the dimensions will go from 1.6 cm on a side to 0.36 cm. Increasing the  $Q$ , then, not only reduces the maximum strain for a given acceleration, but also significantly reduces the size of the device. The deleterious effects of a high  $Q$  suspension, such as nonlinear response near the resonant frequency and ringing, must be dealt with in other areas of the design.

Given the requirements of a particular application in terms of the required noise floor, resonant frequency and  $Q$  of the suspension, thermal noise in the proof mass motion was found to constrain the accelerometer design by requiring a minimum allowable proof mass. The spring design was additionally constrained by requirements of robustness in the presence of large accelerations experienced by an inertial grade accelerometer. In the next section, the ability to take advantage of low thermal noise in a precision accelerometer is considered.

#### 4. ACCELEROMETER SENSITIVITY AND SUSPENSION STIFFNESS

Using a suspension designed for low thermal noise, it is possible to construct a sensitive accelerometer, provided the position sensor has adequate sensitivity. The responsivity of the

accelerometer is given in **equation 5**. At frequencies well below the resonance, the deflection of the proof mass is given by

$$s = \frac{a}{\omega_r^2} \quad \text{for } \omega \ll \omega_r \quad (10)$$

According to this relationship, the resonant frequency of the suspension is related to the stiffness, and determines the deflection,  $s$ , experienced for a given acceleration,  $a$ . Note that replacing the acceleration in equation 10 with a noise density (measured in  $g/\sqrt{\text{Hz}}$ ) will give a noise density for position measurement (measured in  $\text{m}/\sqrt{\text{Hz}}$ ). In figure 5, this relationship is plotted for several different resonant frequencies. The thermal noise floor discussed in the example of the last section,  $10^{-7} g/\sqrt{\text{Hz}}$ , corresponds to a position transducer sensitivity of  $2 \times 10^{-4} \text{ \AA}/\sqrt{\text{Hz}}$  for a resonant frequency of 1 kHz. Measuring deflections with this sensitivity is challenging, particularly for a small instrument. The two most sensitive displacement transducers which have been used for small accelerometers are based on electron tunneling and capacitance measurements of the distance between two electrodes.

Electron tunneling transducers are among the most sensitive displacement sensors available, with a reported sensitivity of  $2.3 \times 10^{-3} \text{ \AA}/\sqrt{\text{Hz}}$  at 10 Hz, and  $2.7 \times 10^{-4} \text{ \AA}/\sqrt{\text{Hz}}$  at 1 kHz.<sup>1,5</sup> While this sensitivity is near the target value in our sample design at higher frequencies, it is not adequate at low

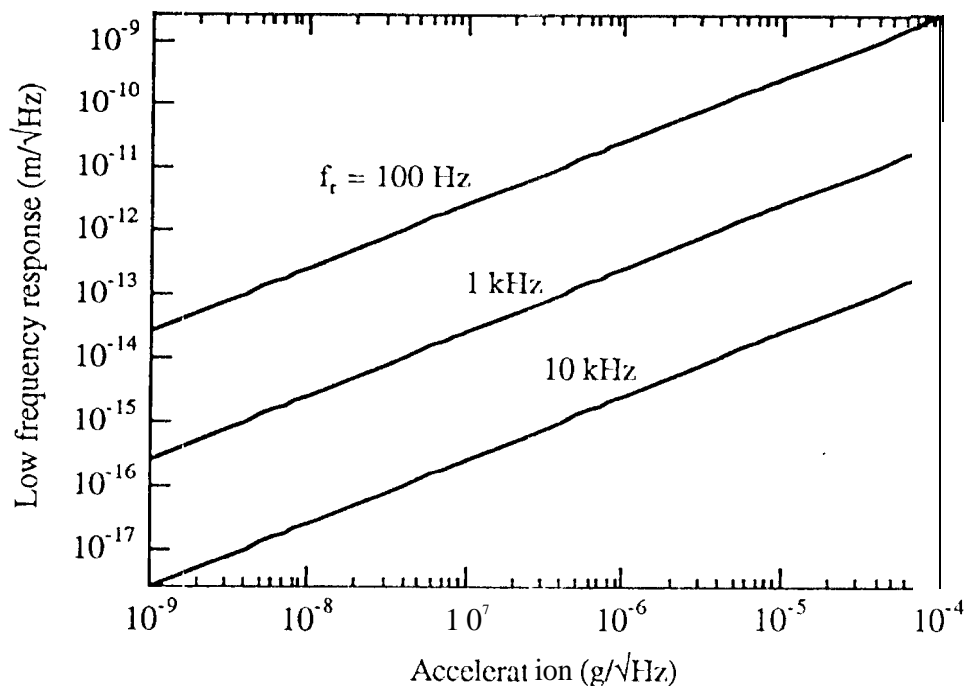


Figure 5: Relationship between the noise equivalent acceleration of an accelerometer and the required sensitivity of a displacement transducer, for three different resonant frequencies. The response is inversely proportional to the square of the resonant frequency (for  $\omega \ll \omega_r^2$ ). As the resonant frequency increases, the required sensitivity of the displacement transducer increases.

frequencies. Stability at low frequencies is important for inertial grade accelerometers, which implies that improvement in the tunnel sensor stability is required to obtain a sensitivity of  $10^{-4} \text{ \AA}/\sqrt{\text{Hz}}$  for the design requirements considered in this example.

High-resolution capacitive displacement transducers have achieved a sensitivity of  $10^{-4} \text{ \AA}/\sqrt{\text{Hz}}$ , which indicates that capacitive techniques are a viable approach. However, these high-resolution systems are large, making them incompatible with small accelerometers, while the capacitive displacement transducers used for micromachined accelerometers are less sensitive than electron tunneling transducers.<sup>3,8</sup> Improved microelectronic circuits are required in order to measure capacitance with sufficient stability to achieve  $10^{-4} \text{ \AA}/\sqrt{\text{Hz}}$  sensitivity at low frequencies. In this context, reducing the size of the accelerometer also reduces the magnitude of the capacitance which must be detected. Assuming that the capacitor gap is 10  $\mu\text{m}$ , the 0.3 gm, 1.6 cm square proof mass discussed in the last section would have a capacitance of 230 pF, whereas the smaller, high Q, 0.36 cm square proof mass would have a capacitance of only 11 pF. Further reduction of the accelerometer size might limit capacitive displacement transducer sensitivity due to the effects of stray capacitance.

## 5. ERROR CORRECTION AND INERTIAL NAVIGATION

Several sources of error must be corrected in order to measure acceleration with high precision for inertial navigation.<sup>9</sup> Various forces on the proof mass arise from the Earth's gravitational field, the spring restoring force, buoyancy, tidal forces (dominated by the moon and sun), rotation of the Earth, and the gravitational attraction of nearby objects (see table 1). Many of the forces tabulated in table 1 are comparable to or greater than the signal being measured. To the extent that these forces are known or calculable, they can be corrected as part of the data analysis. The accuracy with which this needs to be done depends on the required sensitivity, while the ability to make these corrections depends on accurate knowledge of the relevant parameters. Consequently, several limitations to error correction exist which affect the final precision of the measurement. Although sophisticated error correction algorithms improve this precision,<sup>9</sup> the tradeoff between complexity and cost of a micromachined accelerometer is important in many applications.

In order to determine the acceleration, the contribution of the Earth's gravitational field must be subtracted from the signal. One important error in correcting for the gravitational acceleration arises from misinterpreting tilt of the accelerometer with respect to the gravitational field as a signal. A tilt error of  $0.01^\circ$  would result in an error of 170  $\mu\text{g}$  in acceleration in the horizontal plane. The Earth's gravitational field varies with position and time, leading to several potential sources of error.<sup>10</sup> Sophisticated models exist for determining the local gravity vector, uncertainties in which represent one possible limitation on the ultimate accuracy of the calculated position. In the field of gravimetry, models of the gravitational field begin with the gravity ellipsoid, which takes into account the variation of gravity with latitude (g changes by approximately 0.1  $\mu\text{g}$  for every 120 meters of north/south displacement). Gravitational anomalies, or deviations from the gravity ellipsoid, have a wide range of magnitudes. Differences in position or elevation result in errors of up to  $5 \times 10^{-3} \text{ g}$ . Mass deviations from a simple model of the Earth result in variations of the order  $5 \times 10^{-4} \text{ g}$  to  $5 \times 10^{-5} \text{ g}$ . Periodic tidal effects account for variations of up to  $3 \times 10^{-7} \text{ g}$ , and long term mass displacements result in variations on the order of  $10^{-8} \text{ g}$  to  $10^{-9} \text{ g}$ .

Force	Magnitude	Limiting Errors
Earth's gravitational field	1 g	Varies with position, time (Gravimetry)  Orientation of sensor
Spring restoring force	0 - 1 g	Temperature dependent modulus of elasticity (in silicon, 60 $\mu\text{g}/\text{K}$ )  Cross sensitivity  Calibration accuracy (scale factor)
Buoyancy	500 $\mu\text{g}$ (Silicon in air)	Air density fluctuations.  Dependence on acceleration.
Earth's rotation (Eötvös correction)	0-150 $\mu\text{g}$ (0-10 m/s)	Dependence on sensor orientation and velocity.
Magnetic forces	-0.5 Gauss field on Earth	Interaction with instrument (e.g., current-carrying wires).  Dependence on position, orientation, time.
Gravity of nearby objects.	1 ng (30 kg object 0.5 m from sensor)	Prohibitively complicated to identify and track all nearby objects.

Table 1: Partial list of error sources for accelerometers in inertial navigation, with approximate magnitudes.

The rotation of the Earth is a source of error in inertial navigation, which is accounted for by the Eötvös correction.<sup>10</sup> This correction requires knowledge of the position, orientation, and velocity of the accelerometer with respect to the Earth's rotation axis. For a relatively modest speed of 10 m/s, the Eötvös correction can be as large as 150  $\mu\text{g}$ .

The spring restoring force is subject to several sources of error, which are critical to the precision of the measurement of acceleration. The calibration of the accelerometer must be corrected for temperature, due to the temperature-dependence of the elastic modulus of the accelerometer suspension, thermal expansion of the components, and temperature-related bias and gain errors in the electronics. The temperature can be dealt with to some degree by investing some mass and power in temperature stabilization, measurement, and correction. However, residual temperature errors after correction are still a limiting factor in the precision of inertial grade accelerometers.

The buoyancy force on the proof mass is a source of error for sensitive accelerometers. The static buoyancy force on a micromachined proof mass in air is given by the ratio of the densities of air to silicon multiplied by the weight of the proof mass. In terms of an equivalent acceleration, this turns out

to be 0.5 mg, assuming the accelerometer is at rest in a 1 g gravitational field at atmospheric pressure. Fluctuations in the density, or air flow around the proof mass, would cause fluctuations in the buoyancy force which would be detected by the accelerometer as an additional noise term. For inertial guidance applications, an **important** property of the buoyancy force is its dependence on the acceleration of the accelerometer package. Assuming that the accelerometer is enclosed (for isolation from variable wind and pressure), the buoyancy force depends on the local acceleration (gravity plus acceleration signal). Changing the orientation of the accelerometer package by 90° in the Earth's gravitational field could result in a buoyancy-related error of 0.5 mg. Evacuation of the accelerometer package would eliminate buoyancy forces entirely as a source of error.

The gravitational attraction of nearby objects is significant only for extremely accurate accelerometers. One of the calibration techniques for precise seismometers, called G-calibration because of its dependence on the universal gravitational constant, utilizes a 30 kg mass, which, at a distance of 0.5 m from the instrument, produces an attractive force of approximately 1 ng.<sup>11</sup>

There are several important sources of inaccuracy which are present in all inertial measurement units, which are not be considered in detail here. These include cross sensitivity, scale factor error, bias error, non-linearity, vibration rectification, input voltage sensitivity, and misalignment of axes. The correction of all of these errors requires a significant amount of calculation, which implies that the acceleration data must be digitized. Digitization errors are particularly important for precision inertial grade accelerometers which require measurement over a large dynamic range. For example, achieving 7 digit precision (0.1 μg in a 1 g background) will depend on achieving 7 digit stability of voltage references and offsets in the electronics, and 7 digit accuracy in determining the various parameters which go into the correction algorithms (orientation, calibration, and initial conditions). The expense of this effort is illustrated by considering that measuring acceleration with 7 digit accuracy requires a 24 bit D/A converter. It is clear that there will be an important tradeoff between accelerometer precision and cost, due to the complexity of the electronics.

## 6. SUMMARY

The performance of micromachined accelerometers for inertial navigation is limited by thermal noise, displacement transducer sensitivity, and a number of error sources, which range from correction for gravitational acceleration to temperature dependence of the modulus of elasticity. Taken together, these limiting factors constrain the mechanical design of the accelerometer and the complexity of the electronics to form tradeoffs between size, sensitivity, and cost. Scaling laws related to thermal noise were discussed in terms of a sample design for a micromachined, inertial-grade accelerometer which had design parameters of a 1 kHz resonant frequency and a noise floor/ sensitivity of  $10^{-7} g/\sqrt{\text{Hz}}$ . Thermal noise was shown to present an important constraint on the size of the accelerometer, and fragility was considered as a further constraint. The relationship between accelerometer response and displacement transducer sensitivity was considered, and it was determined that displacement transducers represent a limiting technology for precision micromachined accelerometers. Finally, error correction for inertial navigation was considered in terms of a tradeoff between sophistication of the electronics and the cost of the accelerometer.

## ACKNOWLEDGMENTS

Many helpful discussions with Bill Kaiser, Tom VanZandt, and Howard Rockstad are gratefully acknowledged. This work was supported by NASA, JPL, Boeing, and BMDO/IST.

## REFERENCES

1. T. R. VanZandt, T. W. Kenny, and W. J. Kaiser, "Novel position sensor technologies for microaccelerometers," *Proc. SPIE* 1694, 165-172 (1992).
2. W. Riethmüller, W. Beneche, U. Schnakenberg, and B. Wagner, "A smart accelerometer with on-chip electronics fabricated by a commercial CMOS process," *Sensors and Actuators A*, 31, 121-124 (1992).
3. F. Rudolf, A. Jornod, J. Bergqvist, and H. Leuthold, "Precision Accelerometers with  $\mu\text{g}$  Resolution," *Sensors and Actuators*, A21-A23, 297-302 (1990).
4. D. M. Murray, "Integration of Accelerometer Data: Filter Analysis and Design Using Riccati Solutions," *IEEE Transactions on Automatic Control*, AC-32, 174-176 (1987).
5. H. K. Rockstad, T. W. Kenny, J. K. Reynolds, W. J. Kaiser, T. R. VanZandt, and T. B. Gabrielson, "A Miniature High-Resolution Accelerometer Utilizing Electron Tunneling," reprinted from DSC—Vol. 40, *Micromechanical Systems*, Eds. D. Cho, J. P. Peterson, A. P. Pisano, and C. Friedrich, Book No. G00743, pp. 41-52 (1992).
6. W. C. Young, *Roark's Formulas for Stress and Strain*, 6th ed., MacGraw-Hill, New York (1989).
7. K. E. Petersen, "Silicon as a Mechanical Material," *Proceedings of the IEEE*, 70, 420-457 (1982).
8. M. Van Paemel, "Interface Circuit for Capacitive Accelerometer," *Sensors and Actuators*, 17, 629-637 (1989).
9. D. M. Gleason, "Extracting Gravity Vectors from the Integration of Global Positioning System and Inertial Navigation System Data," *Journal of Geophysical Research*, 97, 8853-8864 (1992).
10. W. Torge, *Gravimetry*, Walter de Gruyter, New York (1989).
11. P. Bernard, J.-F. Karczewski, M. Morand, B. Dole, and B. Romanowicz, "The G-Calibration: A New Method for an Absolute *In Situ* Calibration of Long-Period Accelerometers, Tested on the Streckeisen instruments of the Geoscope Network," *Bulletin of the Seismological Society of America*, 81, 1360-1372 (1991).